

Necessity of Standardizing the Definition of QBO Phases

Ke Wei (✉ weike@mail.iap.ac.cn)

Institute of Atmospheric Physics, Chinese Academy of Sciences <https://orcid.org/0000-0002-7616-3493>

Wen Chen

Institute of Atmospheric Physics, Chinese Academy of Sciences

Jiao Ma

Institute of Atmospheric Physics, Chinese Academy of Sciences

Ting Wang

Institute of Atmospheric Physics, Chinese Academy of Sciences

Research Article

Keywords: Necessity of standardizing, definition, QBO phases, mysterious and fascinating natural phenomena, period, downward, stratosphere

Posted Date: July 14th, 2021

DOI: <https://doi.org/10.21203/rs.3.rs-667074/v1>

License: © ⓘ This work is licensed under a Creative Commons Attribution 4.0 International License.

[Read Full License](#)

Abstract

As one of the most mysterious and fascinating natural phenomena, the quasi-biennial oscillation (QBO) has an extraordinary period of ~ 28 months and features alternative westerly and easterly propagating downward from the upper to the lower stratosphere. The QBO is also one of the most important interannual variabilities in the atmosphere, and has dynamical influences on global circulation from the troposphere to the mesosphere, from the tropics to the poles. It also modulates the distribution of chemical constituents such as ozone and methane, and influences tropical cyclone genesis over tropical oceans. The global effect of the QBO is believed to depend on its phase and structure. However, existing definitions of the phase and strength of the QBO remain ambiguous. Previous studies considered tropical zonal winds at 70, 50, 45, 40, 30, 20, and/or 10 hPa, disregarding the propagating characteristic of the QBO in the equatorial stratosphere. In this study, we point out that the definition of the QBO can influence the interpretation of the dynamical effect and decadal variation of the QBO. Therefore, the definition of QBO phases considering the propagating characteristics of the QBO needs to be urgently standardized. By dividing the QBO evolution into multiple phases instead of only two (westerly and easterly), a deeper insight into the dynamics of the QBO, particularly its global effects, may be obtained.

1. Introduction

Featuring the largest interannual variation in the atmosphere, the quasi-biennial oscillation (QBO) has been the most important and interesting phenomena since its discovery in the early 1960s (Reed et al., 1961; Veryard and Ebdon, 1961). It is characterized by alternative westerly and easterly propagating downward from the upper stratosphere to the lower stratosphere, straddling the equator. Varying between 24 to 36 months, averaging ~ 28 months, the period of the QBO is unlike that of any other known climate phenomenon on the Earth and puzzled the scientific community in the early era after its discovery. The characteristics, dynamical mechanism, influence, and model simulation of the QBO and its application in short-term climate prediction have been extensively studied (Baldwin et al., 2001).

Understanding the phases of the QBO (westerly or easterly) is important for investigating its influences and operational application. However, existing means of determining the state and strength of the QBO remain ambiguous. Previous studies have considered equatorial zonal winds at 70, 50, 45, 40, 30, 20, and 10 hPa (Table 1). Holton and Tan (1980) defined the QBO phase using the equatorial zonal wind at 50 hPa over Balboa (9°N). Thereafter, numerous studies used the level of 50 hPa to determine the QBO phases, such as the 50-hPa Singapore (1.22°N) zonal wind (Hamilton, 1993; Huangfu et al., 2019; Kretschmer et al., 2018), the zonal-mean 10°S – 10°N area-averaged zonal wind at 50 hPa (Garfinkel and Hartmann, 2008; Yoo and Son, 2016), and the 5°S – 5°N area-averaged zonal wind at 50 hPa (e.g., Inoue and Takahashi, 2013; Inoue et al., 2011; Klotzbach et al., 2019; Lu et al., 2008; Lu et al., 2014; Mitchell et al., 2011). Maintaining consistency with Holton and Tan (1980), more studies used the equatorial zonal-mean zonal wind at 50 hPa (e.g., Chen and Li, 2007; Chen et al., 2004; Thompson et al., 2002; Wei et al., 2007).

Table 1
Description of typical QBO indices.

Levels	Defining variable(s), methods	Reference
70 hPa	70 hPa Singapore (1.4°N) zonal wind	Liess and Geller (2012)
50 hPa	50 hPa Balboa (9°N) zonal wind	Holton and Tan (1980)
50 hPa	50-hPa Canton Island (2.8°S), Gan Island (0.7°S) or Singapore (1.4°N) zonal wind	Hamilton (1993); Klotzbach et al. (2019); Kretschmer et al. (2018)
50 hPa	Zonal mean, 10°S–10°N zonal wind at 50 hPa	Garfinkel and Hartmann (2008); Yoo and Son (2016)
50 hPa	5°S–5°N area-averaged zonal wind at 50hPa	Inoue and Takahashi (2013); Inoue et al. (2011); Lu et al. (2014); Mitchell et al. (2011) ; Klotzbach et al. (2019)
50 hPa	Equatorial zonal-mean zonal wind at 50 hPa	Chen and Li (2007); Chen et al. (2004); (Lu et al., 2008); Thompson et al. (2002); Wei et al. (2007)
45 hPa	Average of 40 and 50 hPa equatorial zonal wind	(Claud et al., 2008; Labitzke, 2005; Labitzke and Van Loon, 1988)
44 hPa	44 hPa equatorial zonal wind	Pascoe et al. (2005); (Ebdon, 1975)
40 hPa	40 hPa Singapore (1.4°N) zonal wind	Dunkerton and Baldwin (1991)
40 hPa	40 hPa (average of 30 and 50 hPa) Singapore zonal wind	Baldwin and O'sullivan (1995)
40 hPa	Equatorial zonal-mean zonal wind at 40 hPa	Ruzmaikin et al. (2005)
30 hPa	Equatorial zonal wind at 30 hPa	Anstey and Shepherd (2008); Attard and Lang (2019); Camp and Tung (2007); Graf et al. (2014); Hu et al. (2018); Huesmann and Hitchman (2003); Labe et al. (2019); Ribera et al. (2003)
20 hPa	Equatorial zonal wind at 20 hPa	(Pissoft et al., 2013; Pogoreltsev et al., 2014); Naoe et al. (2017)
10 hPa	Zonal wind at 10 hPa	Bushell et al. (2020); Pena-Ortiz et al. (2010)
10, 20, 30, 50, and 70 hPa	Multiple-wind QBO index using zonal winds at multiple levels	Elsbury et al. (2021); Huesmann and Hitchman (2001)

Levels	Defining variable(s), methods	Reference
10, 20, 40 and 70 hPa	Multiple-wind QBO index using zonal winds at multiple levels	Garfinkel et al. (2012)
10 and 70 hPa	Vertical shear of zonal wind between 10 and 70 hPa	Pang and Wu (2002)
30 and 50 hPa	Vertical shear of zonal wind between 30 and 50 hPa	Attard and Lang (2019)
30 and 70 hPa	Vertical shear of tropical-mean (10° S–10° N) zonal wind between 30 and 70 hPa	Wang et al. (2021)
50 and 70 hPa	Vertical shear of zonal wind between 50 and 70 hPa	Huesmann and Hitchman (2001)
50 and 25 hPa	Vertical shear of zonal wind between 25 and 50 hPa	Neu et al. (2014)
25 hPa	Wind shear at 25 hPa (~ 25 km)	Pahlavan et al. (2021)
Multiple levels	Two principal components (PCs) of the zonal mean zonal wind	Baldwin and Dunkerton (1998); Crooks and Gray (2005); Rao and Ren (2018); Blume and Matthes (2012)
Multiple variables	MTM-SVD methods	Pena-Ortiz et al. (2008b); Ribera et al. (2004); Ribera et al. (2003)
Multiple levels	EOF analysis for determining multiple phases	Baldwin and Dunkerton (1998); Gray et al. (2018); Wallace et al. (1993)

To represent the QBO amplitude and phase, Dunkerton and Baldwin (1991) used equatorial zonal wind at 40 mb in Singapore and examined QBO-associated planetary-wave Eliassen-Palm fluxes in boreal winter. Subsequently, Baldwin and O'sullivan (1995) used the DJF average of 40-hPa (average of 30 and 50 hPa) Singapore zonal wind. Other studies have also used the equatorial zonal-mean zonal wind at 40 hPa (Ruzmaikin et al., 2005). Some studies compromised it at 45 hPa (average of 40 and 50 hPa) (Claud et al., 2008; Labitzke, 2005; Labitzke and Van Loon, 1988) or 44 hPa (Ebdon, 1975; Pascoe et al., 2005).

The most intense QBO signal has been observed at around 30 hPa (Mann and Park, 1999; Ribera et al., 2003); therefore, equatorial 30-hPa zonal-mean zonal winds are also frequently used (Anstey and Shepherd, 2008; Attard and Lang, 2019; Camp and Tung, 2007; Graf et al., 2014; Hu et al., 2018; Labe et al., 2019; Ribera et al., 2003). Some studies have also considered the maximum QBO amplitude at around

20 hPa or 30 km (Ebdon, 1975; Huesmann and Hitchman, 2003; Pascoe et al., 2005) and used equatorial zonal winds at these levels (Naoe et al., 2017; Pisoft et al., 2013; Pogoreltsev et al., 2014). The phase of the QBO is also determined by zonal winds at 10 hPa (Bushell et al., 2020; Pena-Ortiz et al., 2010).

Some studies considered the QBO feature of the vertical shear of zonal wind in the equatorial lower stratosphere, and adopted the equatorial vertical zonal wind shear as the QBO index, such as the equatorial wind shear between 10 hPa and 70 hPa (Pang and Wu, 2002), the equatorial zonal wind shear between 30 and 50 hPa (Attard and Lang, 2019), the tropical-mean (10° S– 10° N) zonal wind difference between 30 hPa and 70 hPa (Wang et al., 2021), the shear between 50 hPa and 25 hPa (Neu et al., 2014), wind shear at 25 hPa (~ 25 km) (Pahlavan et al., 2021), and 50–70 hPa zonal mean wind shear (Collimore et al., 2003; Fadnavis et al., 2014; Huesmann and Hitchman, 2001).

There are no unique definitions for the QBO phase with the equatorial westerly and easterly propagating periodically from the upper stratosphere all the way down to the lower stratosphere. Therefore, the study of the extratropical QBO signal can be optimized according to the research objective by selecting a specific optimal level to define the QBO phase. Baldwin and Dunkerton (1998) found that the strongest extratropical Northern Hemisphere (NH) QBO signal can be obtained by considering the equatorial QBO at ~ 40 hPa, while that of the Southern Hemisphere (SH) can be obtained using a level near 25 hPa. Using wind anomalies at 10, 20, 40, and 70 hPa, Garfinkel et al. (2012) demonstrated that extratropical circulation anomalies show different patterns with QBO classification at different levels. This implies that the sensitivity of the selected definition of the QBO phase should be considered when investigating the influence of the QBO on extratropical circulation.

The empirical orthogonal function (EOF) has also been applied to obtain QBO time series. In general, the two principal components (PCs) of zonal-mean zonal winds are adopted (Baldwin and Dunkerton, 1998; Crooks and Gray, 2005; Rao and Ren, 2018). Meanwhile, in order to extract the evolution of the QBO through a complete cycle, the multitaper frequency-domain singular value decomposition (MTM-SVD) (Pena-Ortiz et al., 2008a; Pena-Ortiz et al., 2008b; Ribera et al., 2004; Ribera et al., 2003) and EOF analysis (Baldwin and Dunkerton, 1998; Gray et al., 2018; Wallace et al., 1993) have been used to obtain different phases of the QBO.

With the extension of various types of observations since the discovery of the QBO and the efforts of Holton and Tan (1980) to investigate the extratropical influence of the QBO, the causal relationship between the QBO and the extratropical winter stratosphere circulation is becoming increasingly more apparent. However, the actual dynamics involved may be difficult to determine or highly unclear because of the ambiguous definitions of the phase and strength of the QBO. Therefore, although challenging, it would be productive for the community to standardize the definitions of the phase and strength of the QBO.

Considering this issue, in this study, the following key objectives were set: (1) demonstrate the discrepancy of QBO signals at different levels; (2) examine the sensitivity of the definitions of the QBO to its extratropical influence, implying a need for a standard definition regarding extratropical QBO signals;

(3) argue that a standard definition is necessary for investigating the mechanism the influence of the QBO; (4) suggest possible approaches toward standardizing the definitions of the QBO.

2. Discrepancy Of Qbo Signals At Different Levels

Figure 1 shows cross correlations between monthly equatorial zonal-mean zonal wind anomalies at various altitudes, using the Japanese 55-year Reanalysis (JRA-55) datasets (Ebita et al., 2011). The wind anomalies were obtained by subtracting the monthly climatology from the original wind field. The dominant features are significant negative correlations between the lower (around 50–70 hPa, ~ 20 km) and higher (around 10–7 hPa, ~ 32 km) stratosphere, indicating a zonally symmetric zonal wind seesaw between the higher and lower stratosphere. As the QBO propagates downward at a speed of approximately 1 km per month (Baldwin et al., 2001; Reed et al., 1961), the distance between the two centers (around 12 km) would be covered in approximately 12 months, leading to the quasi-biennial feature of the QBO. If the equatorial wind anomalies propagate downward at a higher speed, for example 2 km per month, the negative correlations between the lower and upper stratosphere, as in Fig. 1, would lead to an oscillation of the quasi-annual period. Therefore, the definition of the QBO index (Pang and Wu, 2002) using the equatorial vertical zonal wind shear (10 hPa minus 70 hPa) takes into account the negative correlation between the higher and lower stratosphere. Based on seasonal mean data, for example spring (March–May mean), summer (June–August mean), autumn (September–November mean), or winter (December–February mean), a similar seesaw relationship can be observed between the higher and lower stratosphere (Figures not shown). We also tested other reanalysis datasets such as ERA5 of the European Center for Medium-Range Weather Forecasts (Hersbach et al., 2020) and MERRA-2 of the National Aeronautics and Space Administration (Gelaro et al., 2017). The results were found to be similar (Figures not shown).

3. Qbo Effects In The Extratropical Stratosphere

Using available gridded data from 1962 to 1972, Holton and Tan (1980) first presented strong evidence that the QBO can affect the extratropical boreal winter stratosphere, with the westerly QBO phase being associated with stronger polar vortex. They then pointed out that springtime zonal wind in the SH stratosphere could also be modulated by the QBO phase. Since then, the term Holton-Tan Oscillation (HTO, or HT relationship) has been coded, and numerous studies adopted their approach using extended data, and the dynamical mechanism was further discussed (e.g., Baldwin and O'sullivan, 1995; Chen et al., 2004; Dunkerton and Baldwin, 1991; Garfinkel et al., 2012; Naito and Hirota, 1997). However, the degree of statistical significance appears to be highly sensitive to the definition of the QBO and the selected level of data.

Figure 2 shows the spatial distribution of the two dominant EOF modes of the boreal stratospheric circulation at 50 hPa and the correlation coefficient (CC) of the equatorial zonal-mean zonal wind with the first two EOF principal components (PCs), indicating the statistical relationship between boreal winter stratospheric circulation and the equatorial zonal-mean zonal wind. The analysis was based on the

JRA55 dataset for the period 1958–2019. To ensure equal weights for equal areas in the EOF analysis, the winter (December to February) gridded data were weighted by the square root of the cosine of the latitude. Then, the winter-mean unweighted anomaly fields were regressed upon the standardized leading PC time series and the regression coefficient as the EOF modes were presented. As the PC time series were standardized to be dimensionless, the values shown in the regression maps represent the anomalies in association with one standard deviation anomaly in the index time series and can be considered typical amplitudes.

The leading EOF (Fig. 2a), which explains 60% of the total variance in the 50-hPa geopotential field, shows a circumpolar pressure seesaw between the polar region and the mid-latitudes. As the geostrophic zonal wind is proportional to the meridional gradient of geopotential height, this EOF describes the variation in the strength of the polar night jet and stratospheric polar vortex (SPV). The seesaw pattern of the extratropical circulation between the polar region and the mid-latitudes actually reflects a basic mode of the atmosphere, i.e., the Northern Annual Mode in the stratosphere (Baldwin and Dunkerton, 1999; Chen and Wei, 2009). The second mode presents a wavy structure of zonal wavenumber 1 (Fig. 2b), which explains approximately 12.3% of the total variance, implying the influence of stationary planetary waves mainly from wavenumber 1.

As HTO reveals that the strength of the polar vortex is positively correlated with the QBO, Fig. 1c indicates that the significant positive CC between PC1 and the equatorial zonal wind is only evident at around 30–70 hPa. If the QBO is defined using equatorial zonal wind around 20 hPa, as in previous studies (e.g., Naoe et al., 2017; Pisoft et al., 2013; Pogoreltsev et al., 2014; Ribera et al., 2003), an insignificant SPV-QBO relationship can be expected. If the QBO is defined using upper stratospheric zonal wind, such as 10 hPa, it is natural to get an opposite HTO relationship. It is worth noting that PC2 is significantly correlated with the equatorial zonal wind at 70 hPa and 10–5 hPa. At 10, 7, and 5 hPa, the CCs between PC2 and the equatorial zonal wind are 0.27, 0.28, and 0.26, respectively, while those between PC1 and the equatorial zonal wind are -0.37, -0.35, and -0.21, respectively. At 70 hPa, the CC between PC2 and the equatorial zonal wind is -0.24, while that between PC1 and equatorial zonal wind is 0.36. Therefore, the selection of the QBO level will determine the correlation between the extratropical circulation EOF mode and the zonal wind as well as the significance of the correlation. If the equatorial vertical zonal wind shear (10 hPa minus 70 hPa) is adopted as the QBO index, it will be significantly correlated with both the extratropical circulation EOF modes. Following Pang and Wu (2002), we firstly standardized the equatorial zonal wind at 10 hPa and 70 hPa, and then used the difference (10 hPa minus 70 hPa) as the QBO index. This index has a CC of 0.34 with SPV-PC1 and a CC of 0.27 with SPV-PC2, which are both significant above the 95% confidence level. Therefore, this QBO index shows a mixed influence on both the strength of the polar vortex and the wavy pattern attributable to wavenumber-1.

The amplitudes of planetary waves in the SH are much smaller than those in the NH. Therefore, the QBO is believed to have the strongest influence during late spring (November), during which the climatologically stronger and longer-lived SH polar vortex weakens and allows the planetary waves to play a relatively important role in the modulation of the strength of winds (Baldwin and Dunkerton, 1998).

Similar to that in the NH, the dominant EOF of the extratropical stratosphere circulation in late spring corresponds to the strength variation of the polar vortex, which accounts for 66.2% of the variance. This pattern is much more symmetrical than its NH counterpart. The second EOF is a wavenumber 1 pattern, which accounts for 14.6% of the total variance. The largest positive CC between PC1 and equatorial zonal wind occurs at 20–30 hPa, confirming the reports of previous studies that the largest extratropical SH influence was observed with the selection of equatorial 25-hPa zonal wind (Baldwin and Dunkerton, 1998; Baldwin et al., 2001). The largest negative CC was observed at around 3–5 hPa. For PC2, the largest positive CC was observed at 50 hPa and the largest negative CC at 10 hPa and 150 hPa. Although PC2 is not significantly related to the equatorial wind in the stratosphere, the vertical distribution of the CC between PC2 and the zonal wind lagged behind that of PC1 by several years. Therefore, for investigating the SH extratropical influence of the QBO, the selection of the QBO definition is an important aspect. Arbitrary selection of a QBO level may lead to a different extratropical stratospheric circulation mode.

The mechanism of the extratropical influence of the QBO has been explored with a focus on the role of planetary waves. Typically, extratropical planetary waves (mainly wavenumber 1 and wavenumber 2 with the largest spatial scales) propagate along the waveguide, i.e., upward from the troposphere mid-latitudes and upward and equatorward in the stratosphere until meeting the critical line (the boundary line between the westerly and easterly), where the wave phase speed is zero. Planetary waves have been suggested to be capable of penetrating into lower latitudes when the tropical stratosphere is in the QBO westerly phase, while the penetration is prevented by a critical line when the tropical stratosphere is in the QBO easterly phase, causing a narrower-than-normal waveguide (Baldwin et al., 2001; Chen et al., 2004; Dunkerton and Baldwin, 1991; Holton and Tan, 1980). A narrower waveguide leads to stronger planetary waves and stronger wave breaking in the extratropical stratosphere, which erodes the stratospheric polar vortex and drags the westerly winds. However, Garfinkel et al. (2012) pointed out that the effect of the mean meridional circulation associated with QBO winds is much more important than the effect of the critical line emphasized in the Holton–Tan mechanism for the polar response to the QBO. However, irrespective of the exact mechanism, the equatorial level modulating the width of the extratropical waveguide or the level of the QBO associated meridional circulation influencing wave propagation at the subpolar latitudes in the upper stratosphere remain unknown.

4. Recommendations

Considering that the QBO winds propagate downward periodically from the upper stratosphere to the lower stratosphere, it may not be sufficient to define the QBO phase using only one specific level. Furthermore, the QBO has a period of ~ 28 months, and after the westerly or easterly is established at one level, it will last for about 14 months. During this process, the QBO index based on one specific level shows the same phase, but the vertical equatorial wind profile exhibits wide changes. Therefore, a more detailed separation of the QBO phase based on the vertical profile of the QBO state is required.

In order to determine the evolution of the QBO through a complete cycle, Wallace et al. (1993) represented the equatorial stratosphere in terms of a vector with radius and phase angle in a two-dimensional phase

space, which is defined by the first two principal components of equatorial stratospheric zonal wind anomalies. During each QBO cycle, the vector completes one nearly circular loop. Similar methods have been adopted in several studies (Baldwin and Dunkerton, 1998; Gray et al., 2018; Wallace et al., 1993). However, the QBO indices were still primarily based on the equatorial zonal wind at one specific level. This emphasizes the necessity of standardizing the definition of the QBO phase.

Following Wallace et al. (1993), the dominant patterns of the tropical stratosphere zonal wind were derived. Due to limitations of their dataset, Wallace et al. (1993) used zonal wind of 7 equatorial levels from three stations. We adopted the tropical zonal-mean zonal wind from the reanalysis (JRA55) data and limited the EOF analysis to the QBO domain (meridional half-width of 15° about the equator and from 70 hPa to 3 hPa). The seasonal cycle was removed from the wind field at each grid point, and a band-pass filter was applied to retain periods between 9 and 48 months. Subsequently, the annual, semiannual, and long-term signals were removed. Moreover, possible influences of the solar cycle were also removed.

Together, EOF1 and EOF2 explain 94.4% of the variance of the 9–48 month band-passed data and are well separated from the remaining EOFs, based on the criteria of North et al. (1982)—EOF3 explains only 4.3% of the variance. The leading EOF structure accounts for 52.7% of the total variance, reflecting the negative correlation between the lower and upper stratosphere. It has a region of westerly anomalies from about 20 hPa to 2 hPa (maximum center ~ 7 hPa), and easterly anomalies from about 100 hPa to 20 hPa (center ~ 50 hPa) with a breaking node around 20 hPa. The second EOF structure accounts for 41.7% of the total variance, representing the variability at the middle stratosphere altitudes. It has a region of easterly anomalies above 5 hPa (center ~ 3 hPa), and westerly anomalies from 50 hPa to 5 hPa (center ~ 20 hPa). This pattern is approximately in quadrature with EOF1. Together, the two EOFs form a degenerate pair, and they can represent the spatially propagating signal of the QBO. Power spectra of the PCs of the leading two EOFs (Figure not shown) indicate that the variance of PC1 and PC2 is concentrated at around 28 months, typically associated with the QBO periodicity. The fractions of the total variance are much preeminent than if the two PC time series behaved as red noise.

The monthly PC1 and PC2 values were obtained by projecting the zonal-mean zonal wind data onto the EOF patterns. The climatology was removed from the zonal wind data before the projection. Following Wallace et al. (1993), the two-dimensional phase space was constructed using monthly PC1 and PC2 indices. Each month is represented by a point determined by the PC1 and PC2 values in this month. The points trace anticlockwise circles around the origin, signifying systematic downward propagation of the QBO. We defined 8 phases (P1 to P8) according to the phase space at 45° intervals, with phases 1 and 5 indicating the positive and negative EOF1, respectively, and phases 3 and 7 indicating the positive and negative EOF2, respectively. By dividing the QBO cycle into 8 phases, detailed information on the modulation of global circulation by the QBO can be obtained.

The entire spatial patterns of atmospheric variability associated with QBO can be explored through the use of composites. Here we applied a composite by taking the average of the observed anomaly field

occurring for the months that fall within each of the 8 phases. The composites for the extended winter season (November to March) and summer season (May to September) are shown in Figs. 5 and 6, respectively. Figure 5a-h shows a complete QBO cycle. In phase 1 (Fig. 5a), equatorial zonal wind shows a negative–positive–negative (“– + –”) pattern from the upper stratosphere to the lower stratosphere. In the upper stratosphere above 3 hPa, the easterly starts to develop, while in the mid stratosphere from 30 to 2 hPa, the westerly reaches its maximum, and in the lower stratosphere below 30 hPa, the easterly dominates. The pattern propagates downward in the tropical region, and the lowest easterly weakens and dissipates in phase 3 (Fig. 5c) and phase 4 (Fig. 5d). By phase 5 (Fig. 5e), the zonal wind pattern has changed into a positive–negative–positive (“+ – +”) pattern from the upper stratosphere to the lower stratosphere. The lowest westerly weakens and dissipates in the following phases (phases 6 and 7). By phase 8 (Fig. 5h), the lower and middle stratosphere is dominated by the easterly, while the westerly prevails in the upper stratosphere.

The QBO has been found to be associated with meridional circulation anomalies (Baldwin et al., 2001; Plumb and Bell, 1982; Takahashi, 1987). The QBO temperature influence shows two nodes around 15° and 50°–60° in the meridional direction that divide the global circulation into three regions: 1) Tropical region—the node around 15° separates the tropical and subtropical regions. Although zonal wind anomalies can further extend poleward to around 20°–30°, the temperature node around 15° is maintained in all QBO phases. In the equatorial region, a temperature maximum occurs in westerly shear zones due to adiabatic warming, which is caused by sinking motion. In easterly shear zones, the opposite holds with minimum temperature associated with rising motion. 2) The subtropical and mid-latitude regions—the node around 50°–60° separates the mid-latitude and polar regions. It is believed that equatorial rising and sinking motions are compensated by the opposing circulation outside the equatorial/tropical region. Therefore, subtropical compensated cooling occurs at the altitudes of tropical warming, and subtropical warming occurs at the altitude of tropical cooling. However, the compensated circulation extends much further even to the subpolar region, which is a much broader meridional circulation than the original estimation. 3) The polar region—circulation anomalies in this region are believed to be related to planetary waves and meridional circulation; however, the exact mechanism is still not very clear.

The equatorial rising and sinking motions and the opposing circulation outside the equatorial/tropical region generate a typical butterfly-like temperature field distribution pattern—resembling a swallowtail butterfly with a forked appearance on the hind wings—in both winter and summer seasons. For example, the temperature composite in Fig. 5e depicts the following feature: 1) in the tropical region, positive anomalies occur in the upper and lower stratosphere, and negative anomalies in the middle stratosphere; 2) in the northern subtropical region, negative anomalies occur in the upper stratosphere, positive anomalies in the middle stratosphere and negative anomalies in the tropopause region; 3) in the southern subtropical region, the pattern is almost symmetrical to that in the northern subtropical region, except that the anomaly amplitude is smaller. This *butterfly* moves downward as the QBO propagates.

5. Extratropical Influences Of The Qbo

5.1. NH stratosphere

It is worth noting that temperature anomalies can be observed in the higher latitudes. Temperature anomalies around the 50°–60° node present a quadrupole temperature anomaly pattern between the polar and mid-latitude regions in the stratosphere in most of the QBO phases. For example, in P1 (Fig. 5a), the two temperature anomaly centers (negative and positive values in the middle and upper stratosphere, respectively) in the middle latitudes are both significantly above the 95% confidence level. A significantly weaker NH polar vortex is observed with easterly anomalies around the polar cap throughout the stratosphere, with a warmer polar region from the tropopause to the middle stratosphere (~ 50 hPa). In the upper stratosphere above 50 hPa, a stronger polar vortex is observed. With the evolution of the QBO, the temperature anomaly centers move poleward and downward in the NH stratosphere. The warmer polar region was confined in the polar region from the tropopause to around 5 hPa, and colder anomalies dominated the polar region above 5 hPa in P2 (Fig. 5b). By P4 (Fig. 5d), the cold anomalies moved to the region below 10 hPa, and the upper stratosphere was influenced by warm anomalies. The comparisons of P1 with P5, P2 with P6, P3 with P7, and P4 with P8 show that linearity is maintained in most regions and in most opposite phases, indicating a dominant linear influence of the QBO on extratropical circulation.

5.2. Comparison between the two hemispheres

The QBO-associated meridional circulation in the winter hemisphere is substantially larger than those in the summer hemisphere. For example, in P1 of the winter season, a significantly colder NH polar vortex can be observed with temperature anomalies of ~ 2.5 K lower than the climatology in the upper stratosphere, while that in the SH polar region is less than 0.8K. In P2 of the winter season, the QBO-associated SH polar temperature anomalies reach ~ 1.0 K, while that of the NH polar temperature anomalies reaches ~ 2.0 K in the mid stratosphere. In P7, the QBO-associated SH polar temperature anomalies reach ~ 1.0 K in the lower stratosphere, while those of the NH polar temperature anomalies reach ~ 3.0 K in the lower stratosphere. The difference is more evident in the zonal-mean zonal wind field. In P1, the zonal wind anomaly center in the NH stratosphere reaches ~ 5 m/s, while that in the SH high latitudes is less than 1 m/s. The QBO-associated zonal wind anomalies in the SH reach their maximum speeds in P3 and P7 at approximately 3 m/s, which is much smaller than their NH counterparts, which approximate 10 m/s. In P1, P2, P4, P5, and P6, the zonal wind anomalies are almost indiscernible in the SH stratosphere.

Similar phenomena occur in the boreal summer season. The QBO-associated zonal wind anomalies are almost imperceptible in all QBO phases throughout the troposphere and stratosphere in the NH polar region, and the high and mid-latitude regions. In contrast, the zonal wind signal is strong in the SH polar region, especially in P1, P4, P5, P6, and P8. Although Baldwin and Dunkerton (1998) indicated that the QBO has the largest influence on the SH polar stratosphere in the SH spring, especially November, the

results of the boreal summer season (May to September) show that the QBO can have significant influences even in other months.

5.3. Summer season anomalies

Since Holton and Tan (1980), the key component linking the equatorial QBO and extratropical circulation has been believed to be planetary waves propagating upward and equatorward from the mid-latitude troposphere. As wave propagation is blocked by stratospheric easterly in the summer season, the extratropical influences of QBO in the summer season, especially on stratospheric circulation, are traditionally ignored. Previous studies on the extratropical circulation of the QBO have mainly focused on the winter season. However, the QBO phase composite in Fig. 6 shows the occurrence of significant temperature anomalies in the NH summer stratosphere. In phase 4, significant negative temperature anomalies could be observed in the mid and high latitudes in the stratosphere. In P8, significant negative temperature anomalies were evident in the mid-latitude upper stratosphere. In comparison, positive temperature anomalies were evident in the polar region in P7. Although the QBO has a very weak influence on the zonal-mean zonal wind in the summer stratosphere, wind anomalies can be observed in the subtropical region in all QBO phases. Moreover, some findings suggest the possible effect of the QBO on the extratropical upper stratosphere in the summer season. In P4, P5, P7, and P8, the upper subpolar stratosphere exhibited a noticeable temperature change.

Regarding the SH summer (Fig. 5), strong negative temperature anomalies could be observed in the polar lower and middle stratosphere in P3, P4, and in the upper stratosphere in P7. Moreover, significant positive temperature anomalies could be discerned in P2 in the middle stratosphere, and in P7 and P8 in the lower stratosphere. The zonal wind anomaly extended to the subtropical region in most phases, with the largest values in the middle and higher latitudes in the stratosphere in P3 and P7. During this period, the QBO exhibited the largest wind anomaly at around 20–30 hPa, confirming the results of Baldwin and Dunkerton (1998) that the SH is best correlated with the QBO index at 20–30 hPa.

5.4. The anomalies at the tropopause

The tropopause and lower stratosphere are other regions worth noting. In both hemispheres and seasons, significant temperature anomalies could be observed around the subtropical tropopause region. When the equatorial lower stratosphere was in the easterly phase (generally QBO P1, P2, P3, and P8), positive T anomalies were observed in both seasons around the subtropical tropopause. Particularly in P1 and P2, positive T anomalies extended poleward to mid-latitudes along the tropopause in both seasons (Fig. 5b and 6b). In contrast, when the equatorial lower stratosphere was in the westerly phases (mainly P4, P5, P6, and P7), negative temperature anomalies dominated the subtropical tropopause in both hemispheres and both seasons. In the boreal summer in the NH, the negative temperature anomalies extended poleward to the polar region in P4, P5, P6, and P7 (Fig. 6d-g), and positive temperature anomalies dominated the tropopause region in P1, P2, and P3 (Fig. 6a-c). The changes in tropopause height and zonal wind shear are considered the key factors modulating convection and tropical cyclone (TC) activity over different tropical oceans (Camargo and Sobel, 2010; Caron et al., 2015; Chan, 1995; Collimore et al.,

2003; Fadnavis et al., 2014; Huangfu et al., 2019; Tao et al., 2018). Therefore, setting a standard definition of the QBO phases may provide a new dynamical perspective on the QBO-TC linkage.

6. Decadal Changes In The Qbo's Effect On The Polar Vortex

The effect of the QBO on the polar vortex is known as HT oscillation. Holton and Tan (1980, 1982) suggested that the wind anomaly configuration of the QBO can modulate planetary wave propagation, leading to variations in the polar vortex. Accordingly, the polar vortex is weak during the easterly QBO phase, usually resulting in major stratospheric sudden warmings (SSWs) (Mcintyre, 1982). Conversely, the polar vortex is less disturbed during the westerly QBO phase. These studies were based on observation and reanalysis data of early times, especially from periods before 1980. Nevertheless, studies involving longer observation times have shown that the HT relationship is unstable (Gray *et al.*, 2001; Lu *et al.*, 2008; Lu *et al.*, 2014; Naito and Hirota, 1997). For example, Lu *et al.* (2008) revealed that the HT relationship was robust during 1958–1976. However, it weakened and reversed during 1977–1997, and the relationship was restored during 1998–2006. Lu *et al.* (2014) suggested that the disruption of the HT effect in 1977–1997 was associated with a change in stratospheric circulation, i.e., a broader and strengthened polar vortex, which may interfere with the modulation of planetary wave propagation by the QBO.

The unstable HT relationship may also reflect the pseudo-periodicity of the QBO. The QBO has alternating wind regimes at intervals of 22–34 months, averaging at periods slightly more than 28 months (Baldwin *et al.*, 2001; Pascoe *et al.*, 2005). Therefore, while winter-mean data, such as those used by Lu *et al.* (2008), are used to study the QBO–polar vortex relationship, the phase of the QBO may vary. As the extratropical circulation effect of the QBO is almost linear, it will be nullified if the QBO phases are evenly distributed. For the winter period (November–March) during 1958–2018, the dominant QBO phases were P1, P4, and P5, corresponding to 13, 9, and 9 winters, respectively. In P1, easterly wind dominates the tropical lower stratosphere, centered at around 50 hPa. In P4, the lower stratosphere is dominated by westerly wind, centered at around 40 hPa. As P5 is the opposite phase of P1, linear correlation/regression will indicate a dominant QBO influence similar to that shown in Figure 5a, i.e., the easterly QBO at 50 hPa associated with a weaker polar jet in the middle stratosphere.

During 1958–1976, the dominant QBO phases were P1, P3, P4, and P5. In P3, the easterly in the tropical lowest stratosphere diminished to zero, and the maximum westerly wind center was at around 20–30 hPa. The westerly was maintained in P3, P4, and P5 at 50 hPa. Accordingly, the linear correlation/regression based on the QBO index at 50 hPa will be similar to that shown in Figure 5a, with the QBO easterly at 50 hPa being associated with a weaker polar jet in the middle stratosphere.

During 1977–1997, the dominant QBO phases were P1 and P6. In P6, the westerly mainly occurred at around 70–100 hPa, but the wind phase was almost neutral at 50 hPa. Therefore, the correlation using

50 hPa QBO could capture the easterly maximum in P1 but interfered by the near-zero winds in P6, leading to a weaker QBO-polar vortex relationship.

During 1998–2018, the dominant QBO phases were P1 and P5, which are two opposite QBO phases. Therefore, the QBO index using equatorial zonal wind at 50 hPa can capture the easterly maximum in P1 and the westerly maximum in P5, leading to a robust correlation between the QBO and stratospheric polar vortex.

As the HT relationship is most unstable in late winter (Lu *et al.*, 2008), Figure 7 shows the same results as Figure 6, except that the averages are taken for February and March only. For late winter, the main QBO phases during 1958–2018 were P1, P4, and P6, with P2 and P5 having moderately higher frequencies. In P1 at 50 hPa, the equatorial zonal wind was in the easterly phase, and it transformed to the westerly phase in P4 and P5. Therefore, the main QBO phases exhibited a tendency to shift towards the opposite distribution, leading to a robust relationship between the 50 hPa QBO index and the polar vortex. During 1958–1976, the maximum frequency was observed in P1 (easterly at 50 hPa), followed by P3 and P5 (easterly at 50 hPa), corresponding to almost opposite QBO phases. However, during 1977–1997, the main phases were P2 and P6, which are transition phases at 50 hPa. The wind speeds were near zero and no clear phase could be identified. Consequently, the correlation between the 50 hPa QBO index and the polar vortex leads to an insignificant relationship. During 1998–2018, the prime QBO phases were P1, P4, and P5, responding to equatorial easterly in P1, and westerly in P4 and P5 at 50 hPa. Therefore, the HT relationship was restored.

7. Discussions

As one of the most important and interesting phenomena in the middle atmosphere, the QBO has attracted the attention of various research communities. However, the means of defining the QBO index remain ambiguous. The equatorial zonal wind at 70, 50, 45, 40, 30, 20, and 10 hPa, as well as the zonal wind shear at various levels, have all been used to define the QBO phases. However, existing definitions have neglected the propagating and pseudo-periodicity characteristics of the QBO. In general, when one QBO phase is established at a specific level, it will last for approximately 12 months. Consequently, the propagation and evolution of the QBO are neglected when the QBO phase at any level is considered. Moreover, a small value of the QBO index at a specific level does not necessarily mean a small QBO amplitude at that time. The index would most likely ignore the QBO wind peak, which may occur at another level at that time.

Considering that the QBO is a propagating and periodic phenomenon, dividing it into only two phases is an extremely simplistic approach. A good example in atmospheric science is the Madden-Julian Oscillation (MJO) (Madden and Julian, 1971, 1972), which is the dominant intraseasonal variability over the tropics and propagates eastward from the Indian Ocean to the central Pacific on the time scale of 30–60 days. The MJO is usually divided into 8 phases (Demott *et al.*, 2015; Donald *et al.*, 2006; Kiladis *et*

al., 2014; Waliser et al., 2009; Wheeler and Hendon, 2004) or more (Maloney and Hartmann, 1998; Maloney and Hartmann, 2000), rather than only 2. When the MJO convective center propagates along the equator, its global influences also change in both location and amplitudes (e.g., Jeong et al., 2005; Ma et al., 2020; Zhang, 2005; Zhang et al., 2009). Similarly, deeper insight into the dynamical mechanism of the global influences of QBO can be obtained by dividing it into more phases.

The influence of the QBO on zonal-mean zonal temperature exhibits a butterfly-shaped distribution pattern in both winter and summer seasons, extending to the subtropical and even polar regions. As the QBO propagates downward, the *butterfly* moves downward. Dividing the QBO into more phases also reveals the effect of the QBO on the subtropical tropopause temperature, which may influence the tropical convection and tropical cyclone activities at some specific phases. These influences warrant further investigation.

The effect of the QBO on extratropical circulation exhibits decadal variations, which is a known characteristic of the unstable relationship between the QBO and polar vortex. These variations are possibly modulated by the solar cycle (Lu et al., 2008) and changes in stratospheric circulation and/or stratosphere–troposphere interaction. Nevertheless, the mechanism can be further understood by considering the uneven distribution of the QBO phases in different periods. As the QBO has a quasi-biennial period, ranging from 22 to 34 months (Baldwin et al., 2001; Bushell et al., 2020; Coy et al., 2016; Huesmann and Hitchman, 2001; Pascoe et al., 2005; Schenzinger et al., 2017), several QBO phases have higher possibility of occurring in some periods, while other phases may dominate the other periods. For the extended winter (November to March) during 1958–1976, P1, P3, P4, and P5 had the largest frequency. During 1977–1997, P1 and P6 were dominant. Moreover, during 1998–2018, the opposite P1 and P5 had the largest frequency. These differences drive the decadal variability of the relationship between the QBO and stratospheric polar vortex.

As the largest interannual signal in the stratosphere, the QBO has dynamical influences on global circulation from the troposphere to the mesosphere, from the tropics to the poles. It also modulates the distribution of chemical constituents, such as ozone and methane, and tropical cyclone genesis over the tropical oceans. A standard definition of QBO phases, with more details on QBO propagation, would shed light on the dynamical mechanism of the global influence of this fascinating phenomenon.

Declarations

Acknowledgments.

The JRA55 data are provided by JMA and are available online at <http://jra.kishou.go.jp/>. We also tested the ERA5 of the European Center for Medium-Range Weather Forecasts from <https://cds.climate.copernicus.eu/cdsapp#!/search?type=dataset> (last access: 20 May 2021), and the MERRA-2 data from the National Aeronautics and Space Administration, Goddard Space Flight Center at https://gmao.gsfc.nasa.gov/reanalysis/MERRA-2/data_access/ (last access: 20 May 2021).

Funding

This research is supported by the Natural Science Foundation of China (Grant No. 4181101164, 41461144001 and 41861144016).

Conflict of interest

The authors declare that they have no conflict of interest.

Availability of data and material

The data is available from the authors upon request

Code availability

The code for diagnostics is available from the authors upon request

References

1. Anstey JA, Shepherd TG (2008) Response of the northern stratospheric polar vortex to the seasonal alignment of QBO phase transitions. *Geophysical Research Letters* 35(22): L22810. <https://doi.org/10.1029/2008gl035721>
2. Attard HE, Lang AL (2019) The Impact of Tropospheric and Stratospheric Tropical Variability on the Location, Frequency, and Duration of Cool-Season Extratropical Synoptic Events. *Monthly Weather Review* 147(2). <https://doi.org/10.1175/mwr-d-18-0039.1>
3. Baldwin MP, O'Sullivan D (1995) Stratospheric Effects of ENSO-Related Tropospheric Circulation Anomalies. *Journal of Climate* 8(4): 649–667.
4. Baldwin MP, Dunkerton TJ (1998) Quasi-biennial modulation of the southern hemisphere stratospheric polar vortex. *Geophysical Research Letters* 25(17): 3343-3346. <https://doi.org/10.1029/98gl02445>
5. Baldwin MP, Dunkerton TJ (1999) Propagation of the Arctic Oscillation from the stratosphere to the troposphere. *Journal of Geophysical Research* 104(D24): 30937-30946. <https://doi.org/10.1029/1999JD900445>
6. Baldwin MP, Gray LJ, Dunkerton TJ, Hamilton K, Haynes PH, Randel WJ, Molton JR, Alexander MJ, Hirota I, Horinouchi T, Jones DBA, Kinnersley JS, Marquardt C, Sato K, Takahashi M (2001) The quasi-biennial oscillation. *Reviews of Geophysics* 39(2): 179-229.
7. Blume C, Matthes K (2012) Understanding and forecasting polar stratospheric variability with statistical models. *Atmospheric Chemistry and Physics* 12(13): 5691-5701. <https://doi.org/10.5194/acp-12-5691-2012>
8. Bushell AC, Anstey JA, Butchart N, Kawatani Y, Osprey SM, Richter JH, Serva F, Braesicke P, Cagnazzo C, Chen CC, Chun HY, Garcia RR, Gray LJ, Hamilton K, Kerzenmacher T, Kim YH, Lott F, McLandress C, Naoe H, Scinocca J, Smith AK, Stockdale TN, Versick S, Watanabe S, Yoshida K, Yukimoto S (2020)

- Evaluation of the Quasi-Biennial Oscillation in global climate models for the SPARC QBO-initiative. Quarterly Journal of the Royal Meteorological Society. <https://doi.org/10.1002/qj.3765>
9. Camargo SJ, Sobel AH (2010) Revisiting the Influence of the Quasi-Biennial Oscillation on Tropical Cyclone Activity. *Journal of Climate* 23(21): 5810-5825. <https://doi.org/10.1175/2010jcli3575.1>
 10. Camp CD, Tung K-K (2007) The influence of the solar cycle and QBO on the late-winter stratospheric polar vortex. *Journal of the Atmospheric Sciences* 64(4): 1267-1283. <https://doi.org/10.1175/jas3883.1>
 11. Caron L-P, Boudreault M, Camargo SJ (2015) On the Variability and Predictability of Eastern Pacific Tropical Cyclone Activity. *Journal of Climate* 28(24): 9678-9696. <https://doi.org/10.1175/jcli-d-15-0377.1>
 12. Chan JCL (1995) Tropical Cyclone Activity in the Western North Pacific in Relation to the Stratospheric Quasi-Biennial Oscillation. *Monthly Weather Review* 123(8): 2567-2571. [https://doi.org/10.1175/1520-0493\(1995\)123<2567:Tcaitw>2.0.Co;2](https://doi.org/10.1175/1520-0493(1995)123<2567:Tcaitw>2.0.Co;2)
 13. Chen W, Li T (2007) Modulation of northern hemisphere wintertime stationary planetary wave activity: East Asian climate relationships by the Quasi-Biennial Oscillation. *Journal of Geophysical Research-Atmospheres* 112(D20), D20120. <https://doi.org/10.1029/2007jd008611>
 14. Chen W, Wei K (2009) Interannual Variability of the Winter Stratospheric Polar Vortex in the Northern Hemisphere and Their Relations to QBO and ENSO. *Advances in Atmospheric Sciences* 26(5): 855-863. <https://doi.org/10.1007/s00376-009-8168-6>
 15. Chen W, Yang L, Huang R, Qiu Q (2004) Diagnostic Analysis of the Impact of Tropical QBO on the General Circulation in the Northern Hemisphere Winter. *Chinese Journal of Atmospheric Science* 28(2): 161-173. (in Chinese)
 16. Claud C, Cagnazzo C, Keckhut P (2008) The effect of the 11-year solar cycle on the temperature in the lower stratosphere. *Journal of Atmospheric and Solar-Terrestrial Physics* 70(16): 2031-2040. <https://doi.org/10.1016/j.jastp.2008.07.010>
 17. Collimore CC, Martin DW, Hitchman MH, Huesmann A, Waliser DE (2003) On the relationship between the QBO and tropical deep convection. *Journal of Climate* 16(15): 2552-2568. [https://doi.org/10.1175/1520-0442\(2003\)016<2552:Otrbtq>2.0.Co;2](https://doi.org/10.1175/1520-0442(2003)016<2552:Otrbtq>2.0.Co;2)
 18. Coy L, Wargan K, Molod AM, McCarty WR, Pawson S (2016) Structure and Dynamics of the Quasi-Biennial Oscillation in MERRA-2. *Journal of Climate* 29(14): 5339-5354. <https://doi.org/10.1175/jcli-d-15-0809.1>
 19. Crooks SA, Gray LJ (2005) Characterization of the 11-year solar signal using a multiple regression analysis of the ERA-40 dataset. *Journal of Climate* 18(7): 996-1015. <https://doi.org/10.1175/jcli-3308.1>
 20. DeMott CA, Klingaman NP, Woolnough SJ (2015) Atmosphere-ocean coupled processes in the Madden-Julian oscillation. *Reviews of Geophysics* 53(4): 1099-1154. <https://doi.org/10.1002/2014rg000478>

21. Donald A, Meinke H, Power B, Maia ADN, Wheeler MC, White N, Stone RC, Ribbe J (2006) Near-global impact of the Madden-Julian Oscillation on rainfall. *Geophysical Research Letters* 33(9), L09704: 4. <https://doi.org/10.1029/2005gl025155>
22. Dunkerton TJ, Baldwin MP (1991) Quasi-biennial modulation of planetary-wave fluxes in the Northern Hemisphere winter. *Journal of the Atmospheric Sciences* 48(8): 1043-1061.
23. Ebdon RA (1975) Quasi-Biennial Oscillation and Its Association with Tropospheric Circulation Patterns. *Meteorological Magazine* 104(1239): 282-297.
24. Ebita A, Kobayashi S, Ota Y, Moriya M, Kumabe R, Onogi K, Harada Y, Yasui S, Miyaoka K, Takahashi K, Kamahori H, Kobayashi C, Endo H, Soma M, Oikawa Y, Ishimizu T (2011) The Japanese 55-year Reanalysis "JRA-55": An Interim Report. *Sola* 7: 149-152. <https://doi.org/10.2151/sola.2011-038>
25. Elsbury D, Peings Y, Magnusdottir G (2021) Variation in the Holton-Tan effect by longitude. *Quarterly Journal of the Royal Meteorological Society* 147(736): 1767-1787. <https://doi.org/10.1002/qj.3993>
26. Fadnavis S, Raj PE, Buchunde P, Goswami BN (2014) In search of influence of stratospheric Quasi-Biennial Oscillation on tropical cyclones tracks over the Bay of Bengal region. *International Journal of Climatology* 34(3): 567-580. <https://doi.org/10.1002/joc.3706>
27. Garfinkel CI, Hartmann DL (2008) Different ENSO teleconnections and their effects on the stratospheric polar vortex. *Journal of Geophysical Research-Atmospheres* 113(D18): 14. <https://doi.org/D18114> 10.1029/2008jd009920
28. Garfinkel CI, Shaw TA, Hartmann DL, Waugh DW (2012) Does the Holton-Tan Mechanism Explain How the Quasi-Biennial Oscillation Modulates the Arctic Polar Vortex? *Journal of the Atmospheric Sciences* 69(5): 1713-1733. <https://doi.org/10.1175/jas-d-11-0209.1>
29. Gelaro R, McCarty W, Suarez MJ, Todling R, Molod A, Takacs L, Randles CA, Darmenov A, Bosilovich MG, Reichle R, Wargan K, Coy L, Cullather R, Draper C, Akella S, Buchard V, Conaty A, da Silva AM, Gu W, Kim G-K, Koster R, Lucchesi R, Merkova D, Nielsen JE, Partyka G, Pawson S, Putman W, Rienecker M, Schubert SD, Sienkiewicz M, Zhao B (2017) The Modern-Era Retrospective Analysis for Research and Applications, Version 2 (MERRA-2). *Journal of Climate* 30(14): 5419-5454. <https://doi.org/10.1175/jcli-d-16-0758.1>
30. Graf HF, Zanchettin D, Timmreck C, Bittner M (2014) Observational constraints on the tropospheric and near-surface winter signature of the Northern Hemisphere stratospheric polar vortex. *Climate Dynamics* 43(12): 3245-3266. <https://doi.org/10.1007/s00382-014-2101-0>
31. Gray LJ, Phipps SJ, Dunkerton TJ, Baldwin MP, Drysdale EF, Allen MR (2001) A data study of the influence of the equatorial upper stratosphere on northern-hemisphere stratospheric sudden warmings. *Quarterly Journal of the Royal Meteorological Society* 127(576): 1985-2004.
32. Gray LJ, Anstey JA, Kawatani Y, Lu H, Osprey S, Schenzinger V (2018) Surface impacts of the Quasi Biennial Oscillation. *Atmospheric Chemistry and Physics* 18(11): 8227-8247. <https://doi.org/10.5194/acp-18-8227-2018>
33. Hamilton K (1993) An examination of observed Southern Oscillation effects in the Northern Hemisphere stratosphere. *Journal of the Atmospheric Sciences* 50(20): 3468-3473.

34. Hersbach H, Bell B, Berrisford P, Hirahara S, Horányi A, Muñoz-Sabater J, Nicolas J, Peubey C, Radu R, Schepers D, Simmons A, Soci C, Abdalla S, Abellan X, Balsamo G, Bechtold P, Biavati G, Bidlot J, Bonavita M, De Chiara G, Dahlgren P, Dee D, Diamantakis M, Dragani R, Flemming J, Forbes R, Fuentes M, Geer A, Haimberger L, Healy S, Hogan RJ, Hólm E, Janisková M, Keeley S, Laloyaux P, Lopez P, Lupu C, Radnoti G, de Rosnay P, Rozum I, Vamborg F, Villaume S, Thépaut J-N (2020) The ERA5 global reanalysis. *Quarterly Journal of the Royal Meteorological Society* 146(730): 1999-2049. <https://doi.org/10.1002/qj.3803>
35. Holton JR, Tan H-C (1980) The influence of the equatorial quasi-biennial oscillation on the global circulation at 50 mb. *Journal of the Atmospheric Sciences* 37(10): 2200-2208.
36. Holton JR, Tan H-C (1982) The quasi-biennial oscillation in the Northern Hemisphere lower stratosphere. *Journal of the Meteorological Society of Japan* 60: 140-148.
37. Hu D, Guan Z, Tian W, Ren R (2018) Recent strengthening of the stratospheric Arctic vortex response to warming in the central North Pacific. *Nature Communications* 9(1): 1697. <https://doi.org/10.1038/s41467-018-04138-3>
38. Huangfu J, Chen W, Jian M, Huang R (2019) Impact of the cross-tropopause wind shear on tropical cyclone genesis over the Western North Pacific in May. *Climate Dynamics* 52(7-8): 3845-3855. <https://doi.org/10.1007/s00382-018-4363-4>
39. Huesmann AS, Hitchman MH (2001) The stratospheric quasi-biennial oscillation in the NCEP reanalyses: climatological structures. *Journal of Geophysical Research* 106(D11): 11859-11874.
40. Huesmann AS, Hitchman MH (2003) The 1978 shift in the NCEP reanalysis stratospheric quasi-biennial oscillation. *Geophysical Research Letters* 30(2), 1048. <https://doi.org/10.1029/2002gl016323>
41. Inoue M, Takahashi M (2013) Connections between the stratospheric quasi-biennial oscillation and tropospheric circulation over Asia in northern autumn. *Journal of Geophysical Research-Atmospheres* 118(19): 10740-10753. <https://doi.org/10.1002/jgrd.50827>
42. Inoue M, Takahashi M, Naoe H (2011) Relationship between the stratospheric quasi-biennial oscillation and tropospheric circulation in northern autumn. *Journal of Geophysical Research-Atmospheres* 116, D24115. <https://doi.org/10.1029/2011jd016040>
43. Jeong JH, Ho CH, Kim BM, Kwon WT (2005) Influence of the Madden-Julian Oscillation on wintertime surface air temperature and cold surges in east Asia. *Journal of Geophysical Research-Atmospheres* 110(D11), D11104. <https://doi.org/10.1029/2004jd005408>
44. Kiladis GN, Dias J, Straub KH, Wheeler MC, Tulich SN, Kikuchi K, Weickmann KM, Ventrone MJ (2014) A Comparison of OLR and Circulation-Based Indices for Tracking the MJO. *Monthly Weather Review* 142(5): 1697-1715. <https://doi.org/10.1175/mwr-d-13-00301.1>
45. Klotzbach P, Abhik S, Hendon HH, Bell M, Lucas C, Marshall AG, Oliver ECJ (2019) On the emerging relationship between the stratospheric Quasi-Biennial oscillation and the Madden-Julian oscillation. *Scientific Reports*(2981). <https://doi.org/s41598-019-40034-6>

46. Kretschmer M, Cohen J, Matthias V, Runge J, Coumou D (2018) The different stratospheric influence on cold-extremes in Eurasia and North America. *npj Climate and Atmospheric Science* 1(1): 44. <https://doi.org/10.1038/s41612-018-0054-4>
47. Labe Z, Peings Y, Magnusdottir G (2019) The Effect of QBO Phase on the Atmospheric Response to Projected Arctic Sea Ice Loss in Early Winter. *Geophysical Research Letters* 46(13): 7663-7671. <https://doi.org/10.1029/2019gl083095>
48. Labitzke K (2005) On the solar cycle-QBO relationship: a summary. *Journal of Atmospheric and Solar-Terrestrial Physics* 67(1-2): 45-54.
49. Labitzke K, van Loon H (1988) Associations between the 11-year solar cycle, the QBO and the atmosphere. I-The troposphere and stratosphere in the Northern Hemisphere in winter. *Journal of Atmospheric and Terrestrial Physics* 50: 197-206.
50. Liess S, Geller MA (2012) On the relationship between QBO and distribution of tropical deep convection. *Journal of Geophysical Research-Atmospheres* 117, D03108. <https://doi.org/10.1029/2011jd016317>
51. Lu H, Baldwin MP, Gray LJ, Jarvis MJ (2008) Decadal-scale changes in the effect of the QBO on the northern stratospheric polar vortex. *Journal of Geophysical Research-Atmospheres* 113: D10114, doi:10.1029/12007JD009647. <https://doi.org/10.1029/2007jd009647>
52. Lu H, Bracegirdle TJ, Phillips T, Bushell A, Gray L (2014) Mechanisms for the Holton-Tan relationship and its decadal variation. *Journal of Geophysical Research-Atmospheres* 119(6): 2811-2830. <https://doi.org/10.1002/2013jd021352>
53. Ma J, Chen W, Nath D, Lan X (2020) Modulation by ENSO of the Relationship Between Stratospheric Sudden Warming and the Madden-Julian Oscillation. *Geophysical Research Letters* 47(15), e2020GL088894. <https://doi.org/10.1029/2020gl088894>
54. Madden RA, Julian PR (1971) Detection of a 40–50 Day Oscillation in the Zonal Wind in the Tropical Pacific. *Journal of the Atmospheric Sciences* 28(5): 702+. [https://doi.org/10.1175/1520-0469\(1971\)028<0702:Doadoi>2.0.Co;2](https://doi.org/10.1175/1520-0469(1971)028<0702:Doadoi>2.0.Co;2)
55. Madden RA, Julian PR (1972) Description of Global-Scale Circulation Cells in the Tropics with a 40–50 Day Period. *Journal of the Atmospheric Sciences* 29(6): 1109+. [https://doi.org/10.1175/1520-0469\(1972\)029<1109:Dogscc>2.0.Co;2](https://doi.org/10.1175/1520-0469(1972)029<1109:Dogscc>2.0.Co;2)
56. Maloney ED, Hartmann DL (1998) Frictional moisture convergence in a composite life cycle of the Madden-Julian oscillation. *Journal of Climate* 11(9): 2387-2403. [https://doi.org/10.1175/1520-0442\(1998\)011<2387:Fmciac>2.0.Co;2](https://doi.org/10.1175/1520-0442(1998)011<2387:Fmciac>2.0.Co;2)
57. Maloney ED, Hartmann DL (2000) Modulation of Eastern North Pacific Hurricanes by the Madden–Julian Oscillation. *Journal of Climate* 13(9): 1451-1460. [https://doi.org/10.1175/1520-0442\(2000\)013<1451:Moenph>2.0.Co;2](https://doi.org/10.1175/1520-0442(2000)013<1451:Moenph>2.0.Co;2)
58. Mann ME, Park J (1999) Oscillatory spatiotemporal signal detection in climate studies: A multiple-taper spectral domain approach. *Advances in Geophysics*, Vol 41 41: 1-131. [https://doi.org/10.1016/s0065-2687\(08\)60026-6](https://doi.org/10.1016/s0065-2687(08)60026-6)

59. McIntyre M (1982) How well do we understand the dynamics of stratospheric warmings. *J Meteor Soc Japan* 60: 37-65.
60. Mitchell DM, Gray LJ, Charlton-Perez AJ (2011) The structure and evolution of the stratospheric vortex in response to natural forcings. *Journal of Geophysical Research-Atmospheres* 116, D15110. <https://doi.org/10.1029/2011jd015788>
61. Naito Y, Hirota I (1997) Interannual variability of the northern winter stratospheric circulation related to the QBO and the solar cycle. *J Meteor Soc Japan* 75: 925-937.
62. Naoe H, Deushi M, Yoshida K, Shibata K (2017) Future Changes in the Ozone Quasi-Biennial Oscillation with Increasing GHGs and Ozone Recovery in CCM1 Simulations. *Journal of Climate* 30(17): 6977-6997. <https://doi.org/10.1175/jcli-d-16-0464.1>
63. Neu JL, Flury T, Manney GL, Santee ML, Livesey NJ, Worden J (2014) Tropospheric ozone variations governed by changes in stratospheric circulation. *Nature Geoscience* 7: 340. <https://doi.org/10.1038/ngeo2138>
64. North GR, Bell TL, Cahalan RF, Moeng FJ (1982) Sampling Errors in the Estimation of Empirical Orthogonal Functions. *Monthly Weather Review* 110(7): 699-706.
65. Pahlavan HA, Fu Q, Wallace JM, Kiladis GN (2021) Revisiting the Quasi-Biennial Oscillation as Seen in ERA5. Part I: Description and Momentum Budget. *Journal of the Atmospheric Sciences* 78(3): 673-691. <https://doi.org/10.1175/jas-d-20-0248.1>
66. Pang X, Wu H (2002) Relationship between Vertical Shear of Zonal Wind in Equatorial Lower Stratosphere and ENSO Variability. *Journal of Nanjing Institute of Meteorology* 25(1): 62-68. (in Chinese)
67. Pascoe CL, Gray LJ, Crooks SA, Juckes MN, Baldwin MP (2005) The quasi-biennial oscillation: Analysis using ERA-40 data. *J Geophys Res* 110: D08105, doi:08110.01029/02004JD004941.
68. Pena-Ortiz C, Garcia-Herrera R, Ribera P, Calvo N (2008a) Hemispheric Asymmetries in the Quasi-biennial Oscillation Signature on the Mid- to High-Latitude Circulation of the Stratosphere. In: L Gimeno, R Garcia-Herrera, R M Trigo (eds) *Trends and Directions in Climate Research*, pp32-49
69. Pena-Ortiz C, Schmidt H, Giorgetta MA, Keller M (2010) QBO modulation of the semiannual oscillation in MAECHAM5 and HAMMONIA. *Journal of Geophysical Research-Atmospheres* 115, D21106. <https://doi.org/10.1029/2010jd013898>
70. Pena-Ortiz C, Ribera P, Garcia-Herrera R, Giorgetta MA, Garcia RR (2008b) Forcing mechanism of the seasonally asymmetric quasi-biennial oscillation secondary circulation in ERA-40 and MAECHAM5. *Journal of Geophysical Research-Atmospheres* 113(D16), D16103. <https://doi.org/10.1029/2007jd009288>
71. Pisoft P, Holtanova E, Huszar P, Kalvova J, Miksovsky J, Raidl A, Zemankova K, Zak M (2013) Manifestation of reanalyzed QBO and SSC signals. *Theoretical and Applied Climatology* 112(3-4): 637-646. <https://doi.org/10.1007/s00704-012-0752-5>
72. Plumb AR, Bell RC (1982) A model of the quasi-biennial oscillation on an equatorial beta-plane. *Quarterly Journal of the Royal Meteorological Society* 108(456): 335-352.

73. Pogoreltsev AI, Savenkova EN, Pertsev NN (2014) Sudden stratospheric warmings: the role of normal atmospheric modes. *Geomagnetism and Aeronomy* 54(3): 357-372. <https://doi.org/10.1134/s0016793214020169>
74. Rao J, Ren RC (2018) Varying stratospheric responses to tropical Atlantic SST forcing from early to late winter. *Climate Dynamics* 51(5-6): 2079-2096. <https://doi.org/10.1007/s00382-017-3998-x>
75. Reed RJ, Campbell W, Rasmussen L, Rogers D (1961) Evidence of a downward-propagating annual wind reversal in the equatorial stratosphere. *Journal of Geophysical Research* 66: 813-818.
76. Ribera P, Pena-Ortiz C, Garcia-Herrera R, Gallego D, Gimeno L, Hernandez E (2004) Detection of the secondary meridional circulation associated with the quasi-biennial oscillation. *Journal of Geophysical Research-Atmospheres* 109(D18112). <https://doi.org/10.1029/2003JD004363>
77. Ribera P, Gallego D, Pena-Ortiz C, Gimeno L, Garcia-Herrera R, Hernandez E, Calvo N (2003) The stratospheric QBO signal in the NCEP reanalysis, 1958-2001. *Geophysical Research Letters* 30(13): 4. <https://doi.org/10.1029/2003GL017131>
78. Ruzmaikin A, Feynman J, Jiang X, Yung YL (2005) Extratropical signature of the quasi-biennial oscillation. *J Geophys Res* 110(D11): D11111, doi:11110.11029/12004JD005382.
79. Schenzinger V, Osprey S, Gray L, Butchart N (2017) Defining metrics of the Quasi-Biennial Oscillation in global climate models. *Geoscientific Model Development* 10(6): 2157-2168. <https://doi.org/10.5194/gmd-10-2157-2017>
80. Takahashi M (1987) A two-dimensional numerical model of the quasi-biennial oscillation. *Journal of the Meteorological Society of Japan* 65(4): 523-536.
81. Tao L, Lan Y, Kong C (2018) Interdecadal variations in the relationship between the intense tropical cyclones over the Western North Pacific Ocean and the ENSO. *Transactions of Atmospheric Sciences* 41(5), 1674-7097(2018)41:5<596:Eyxbtp>2.0.Tx;2-p: 596-607.
82. Thompson DWJ, Baldwin MP, Wallace JM (2002) Stratospheric Connection to Northern Hemisphere Wintertime Weather: Implications for Prediction. *Journal of Climate* 15(12): 1421-1428.
83. Veryard RG, Ebdon RA (1961) Fluctuations in tropical stratospheric winds. *Meteor Mag* 90: 125-143.
84. Waliser D, Sperber K, Hendon H, Kim D, Wheeler M, Weickmann K, Zhang C, Donner L, Gottschalck J, Higgins W, Kang IS, Legler D, Moncrieff M, Vitart F, Wang B, Wang W, Woolnough S, Maloney E, Schubert S, Stern W, Clivar Madden-Julian O (2009) MJO Simulation Diagnostics. *Journal of Climate* 22(11): 3006-3030. <https://doi.org/10.1175/2008jcli2731.1>
85. Wallace JM, Panetta RL, Estberg J (1993) Representation of the Equatorial Stratospheric Quasi-Biennial Oscillation in EOF Phase Space. *Journal of the Atmospheric Sciences* 50(12): 1751-1762. [https://doi.org/10.1175/1520-0469\(1993\)050<1751:ROTESQ>2.0.CO;2](https://doi.org/10.1175/1520-0469(1993)050<1751:ROTESQ>2.0.CO;2)
86. Wang L, Wang L, Chen W, Huangfu J (2021) Modulation of winter precipitation associated with tropical cyclone of the western North Pacific by the stratospheric Quasi-Biennial oscillation. *Environmental Research Letters* 16(5), 054004. <https://doi.org/10.1088/1748-9326/abf3dd>
87. Wei K, Chen W, Huang RH (2007) Association of tropical Pacific sea surface temperatures with the stratospheric Holton-Tan Oscillation in the Northern Hemisphere winter. *Geophysical Research*

Letters 34(16): L16814,

doi:16810.11029/12007GL030478. <https://doi.org/10.1029/2007gl030478>|issn 0094-8276

88. Wheeler MC, Hendon HH (2004) An all-season real-time multivariate MJO index: Development of an index for monitoring and prediction. *Monthly Weather Review* 132(8): 1917-1932. [https://doi.org/10.1175/1520-0493\(2004\)132<1917:Aarmmi>2.0.Co;2](https://doi.org/10.1175/1520-0493(2004)132<1917:Aarmmi>2.0.Co;2)
89. Yoo C, Son S-W (2016) Modulation of the boreal wintertime Madden-Julian oscillation by the stratospheric quasi-biennial oscillation. *Geophysical Research Letters* 43(3): 1392-1398. <https://doi.org/10.1002/2016gl067762>
90. Zhang C (2005) Madden-Julian Oscillation. *Rev Geophys* 43, 2004RG000158: 36.
91. Zhang L, Wang B, Zeng Q (2009) Impact of the Madden-Julian Oscillation on Summer Rainfall in Southeast China. *Journal of Climate* 22(2): 201-216. <https://doi.org/10.1175/2008jcli1959.1>

Figures

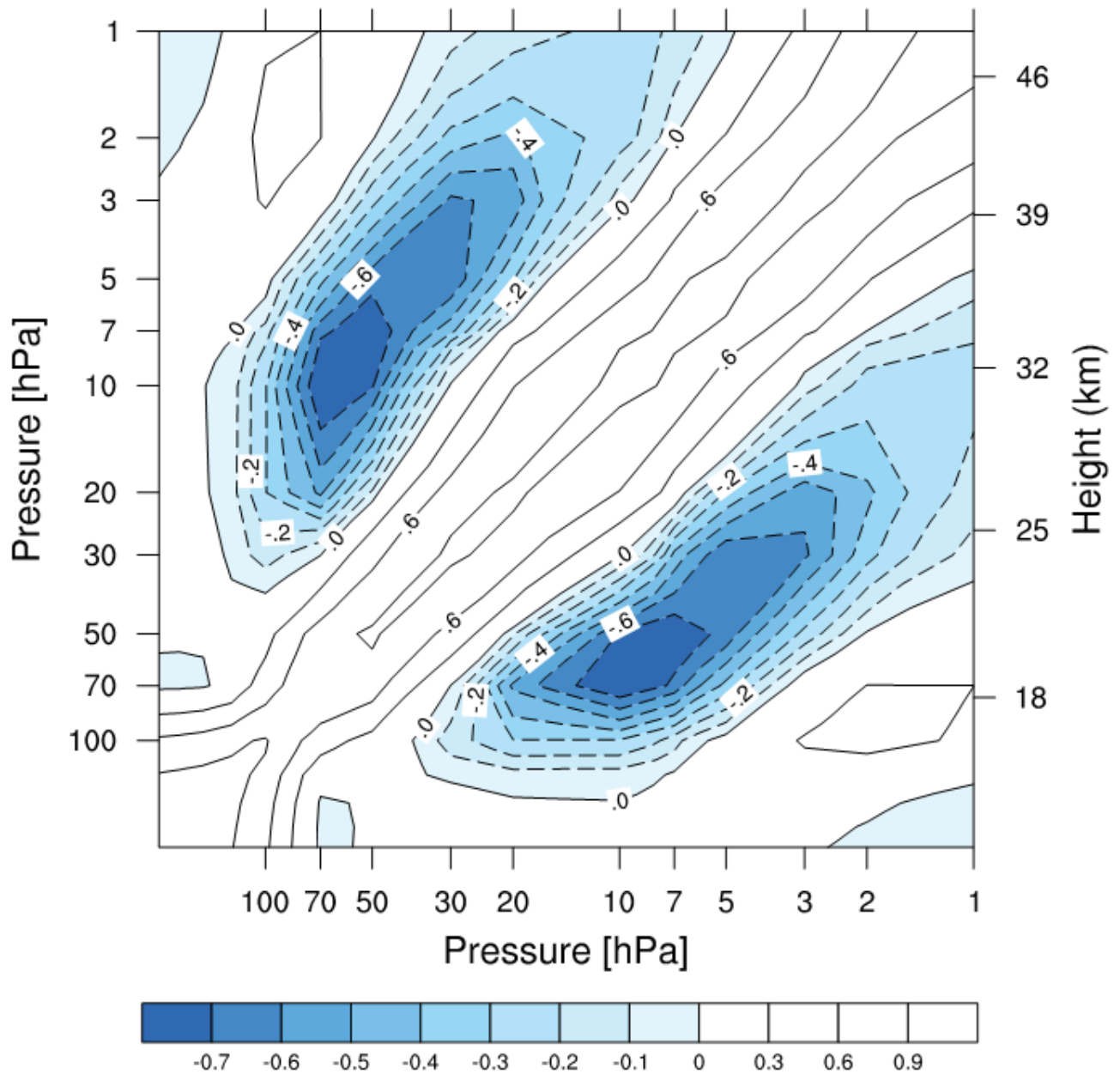


Figure 1

Cross correlation between monthly equatorial zonal-mean zonal wind anomalies (1958–2018, the annual cycle is removed by subtracting the climatology) at different levels using the JRA55 datasets. The contour interval is 0.1 for negative values and 0.3 for positive values. Note that the figure is symmetric about the diagonal.

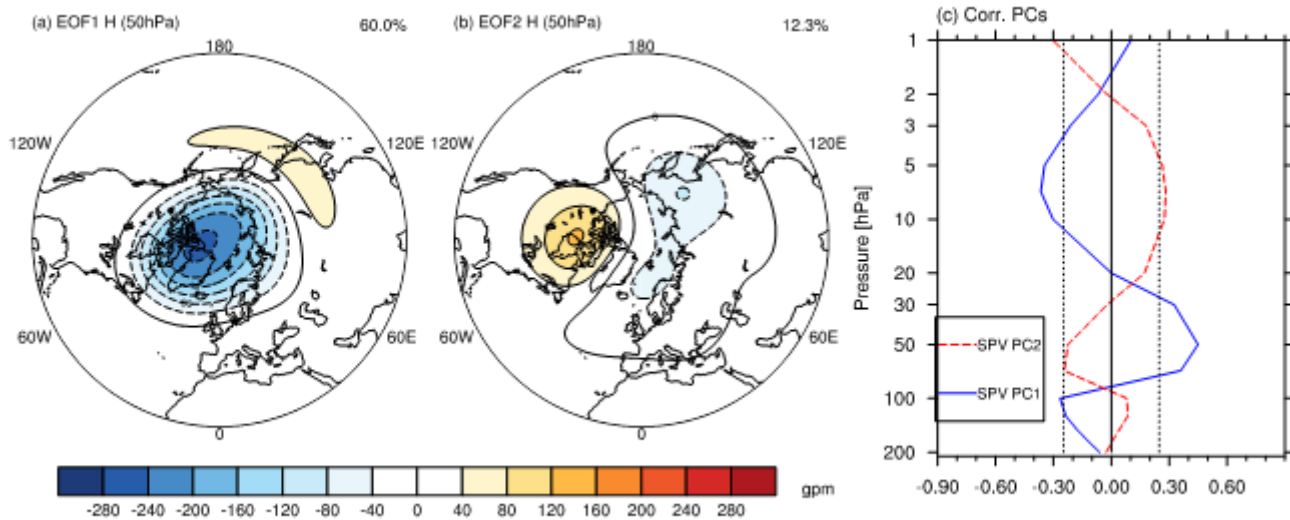


Figure 2

Spatial distribution of (a) EOF1 and (b) EOF2 of the 50-hPa geopotential height field north of 20°N in the Northern Hemisphere winter (December–February) during 1979–2014 (from the JRA55 datasets). The contour interval is 40 gpm. (c) Vertical distribution of the correlation coefficient of the equatorial zonal-mean zonal wind with the first two EOF principal components. The solid blue line is for PC1, and the red dashed line is for PC2.

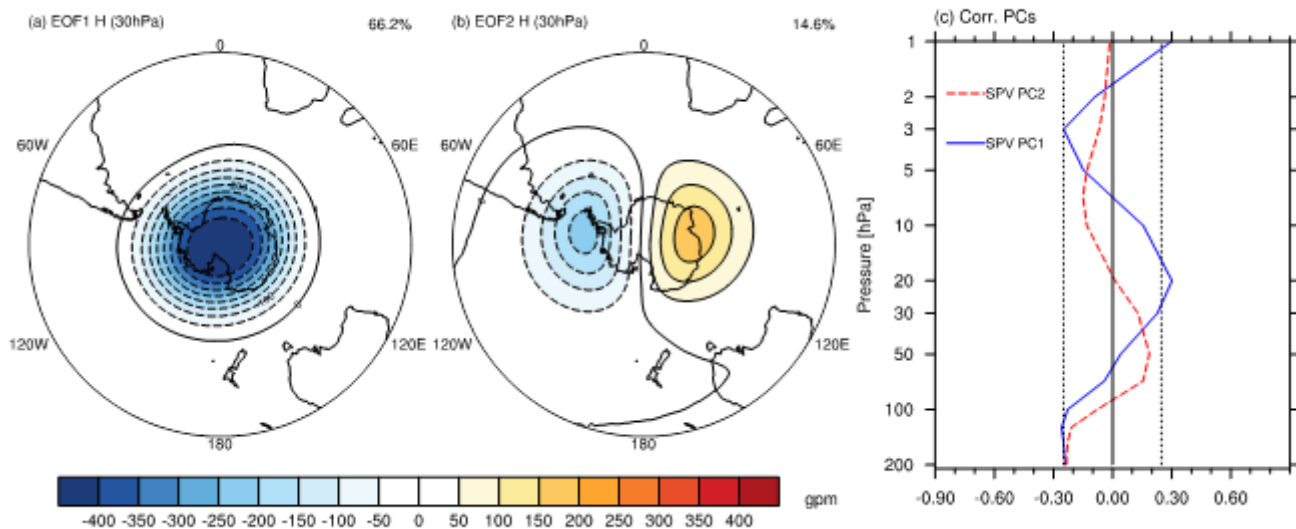


Figure 3

Same as Fig. 2, except for the 30-hPa geopotential height field south of -20°S in the Southern Hemisphere in late spring (November).

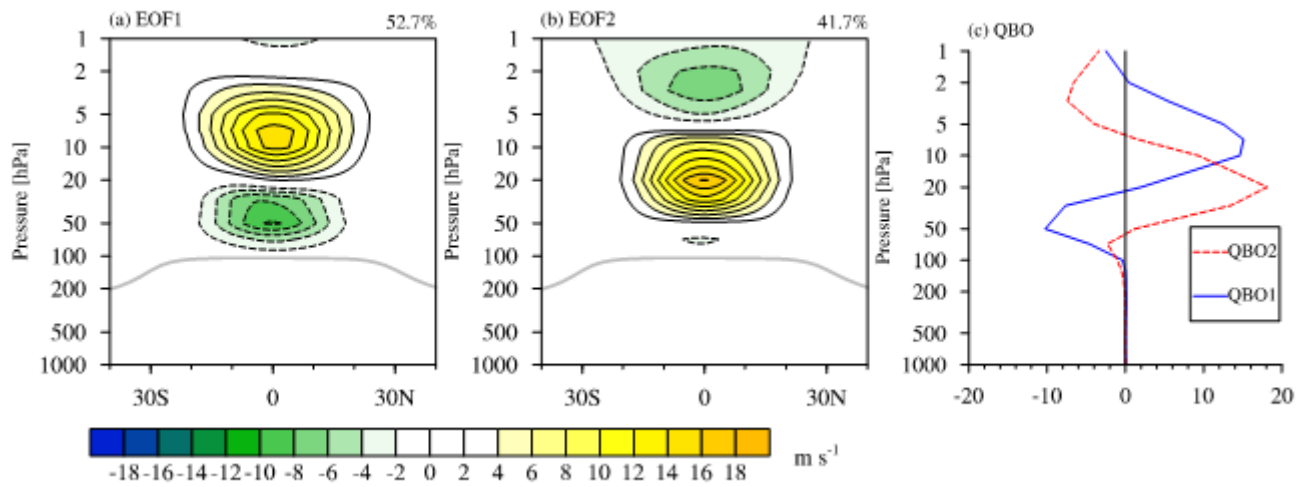


Figure 4

The leading first (a) and second (b) EOF of the tropical zonal-mean zonal wind field in the stratosphere (15°S to 15°N, 70hPa to 1hPa). (c) Zonal wind profile corresponding to EOF1 and EOF2 at the equator.

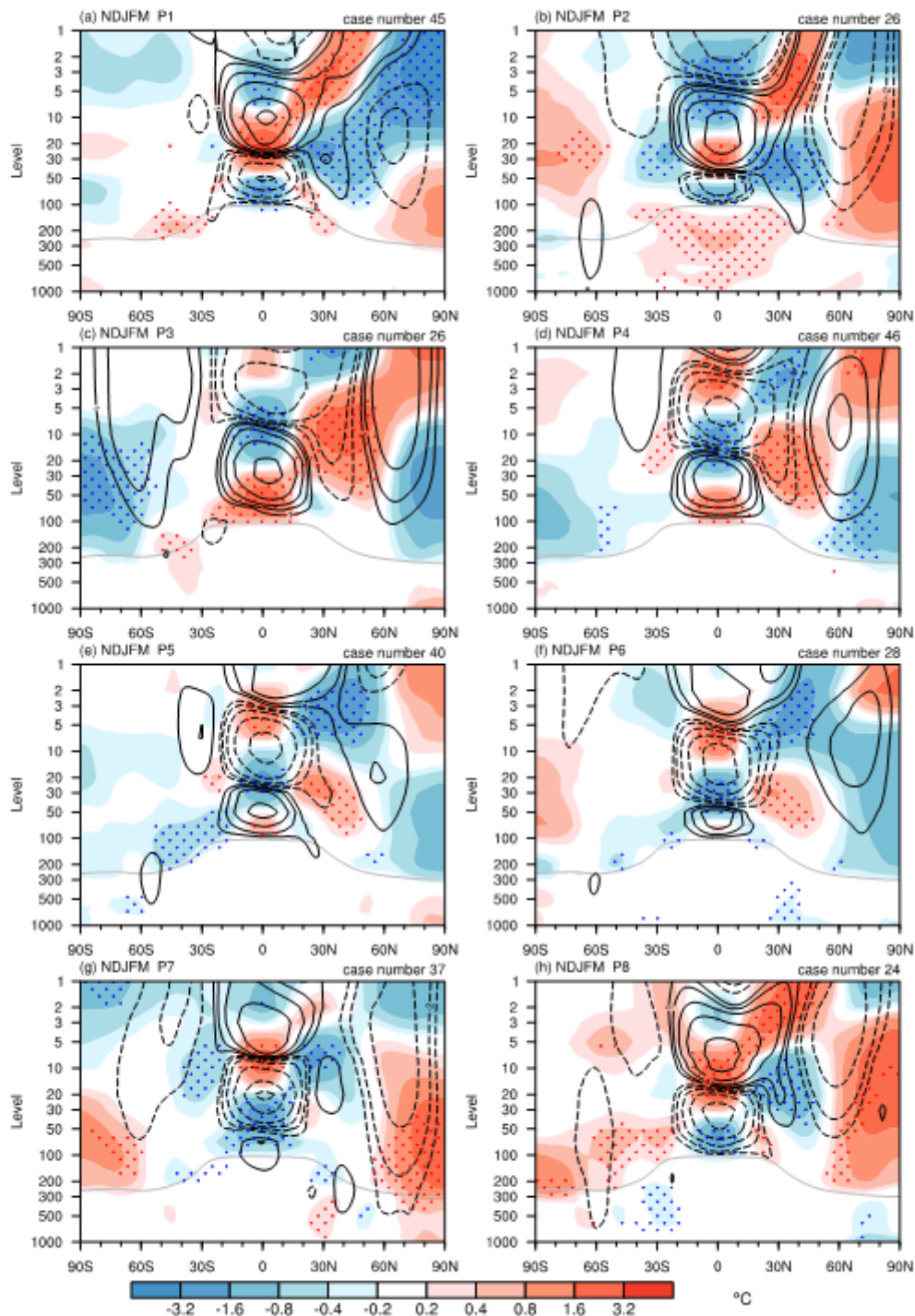


Figure 5

Composites of zonal-mean zonal wind (contours) and temperature (shadings) anomalies with respect to the quasi-biennial oscillation (QBO) phases for the extended winter season (November to March). Contours are drawn at $\pm 1, \pm 2, \pm 4, \pm 8, \pm 16, \pm 24,$ and ± 32 m/s. The zero lines are omitted. Stippling shows the significant region above the 95% confidence level for the zonal-mean zonal temperature regression.

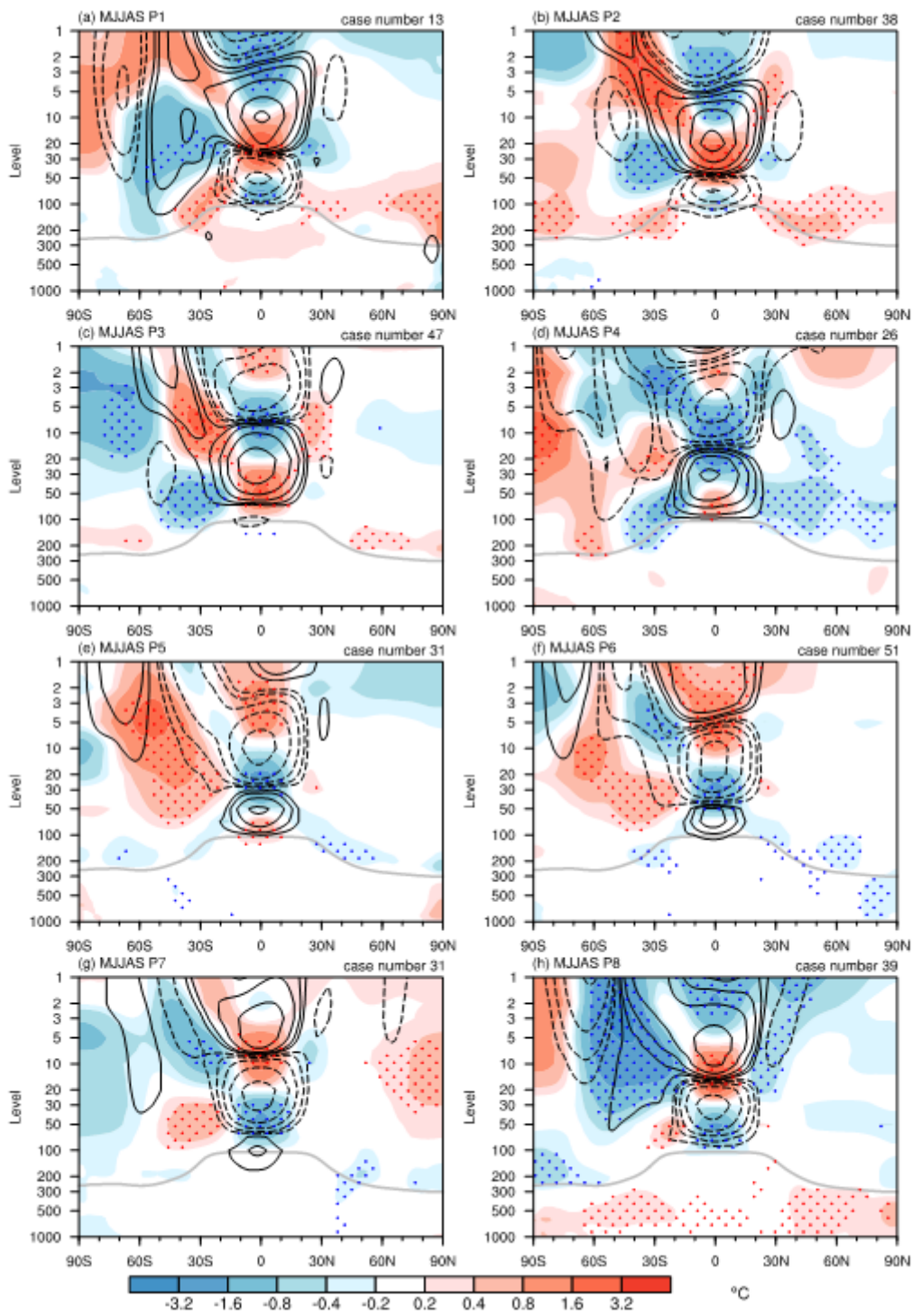


Figure 6

Same as Fig. 5 but for the summer season (June to September)

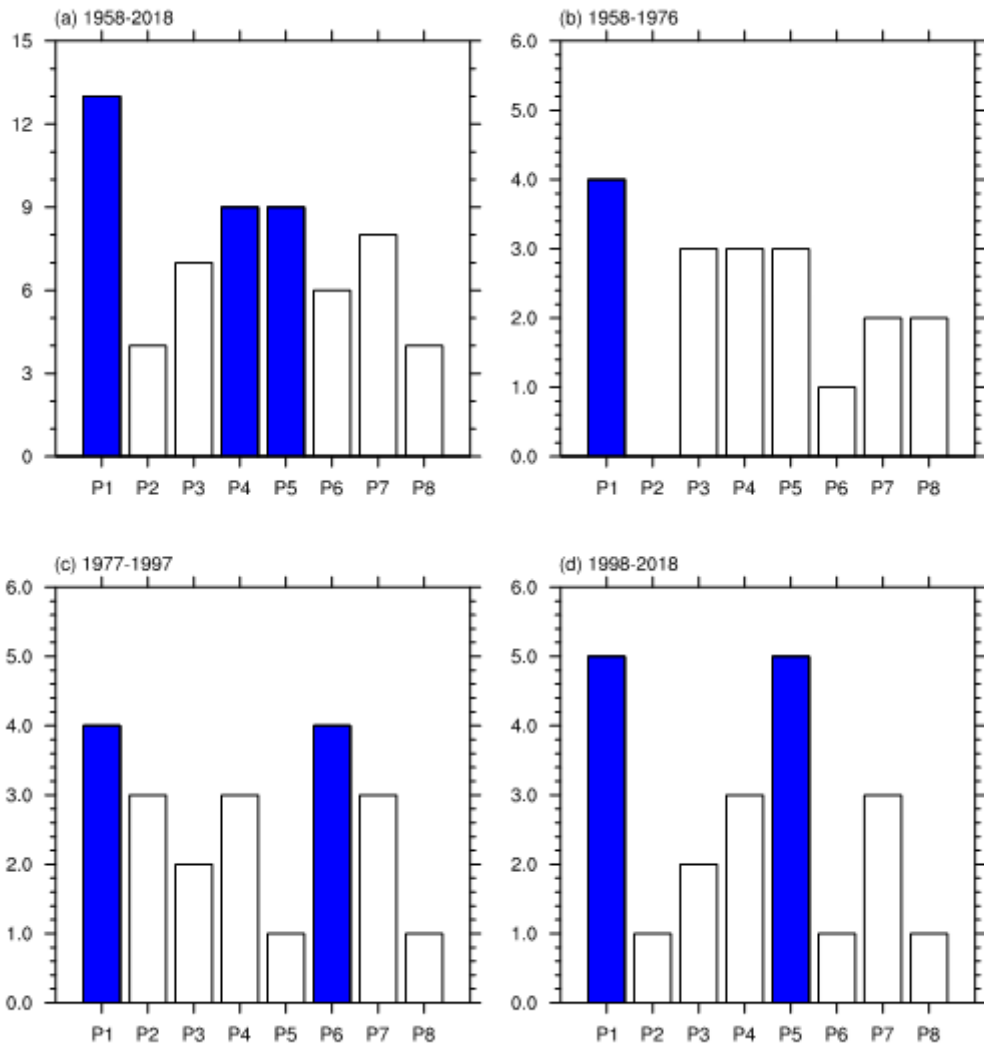


Figure 7

Histogram showing the frequency distribution of the phases of the QBO for the period of (a) 1958–2018, and sub-periods of (b) 1958–1976, (c) 1977–1997, and (d) 1998–2018, at 45° intervals (P1, P2, ..., P8) expressed as a fraction of a cycle. The QBO phase is constructed using zonal-mean zonal wind averaged over the extended winter periods (November to March).

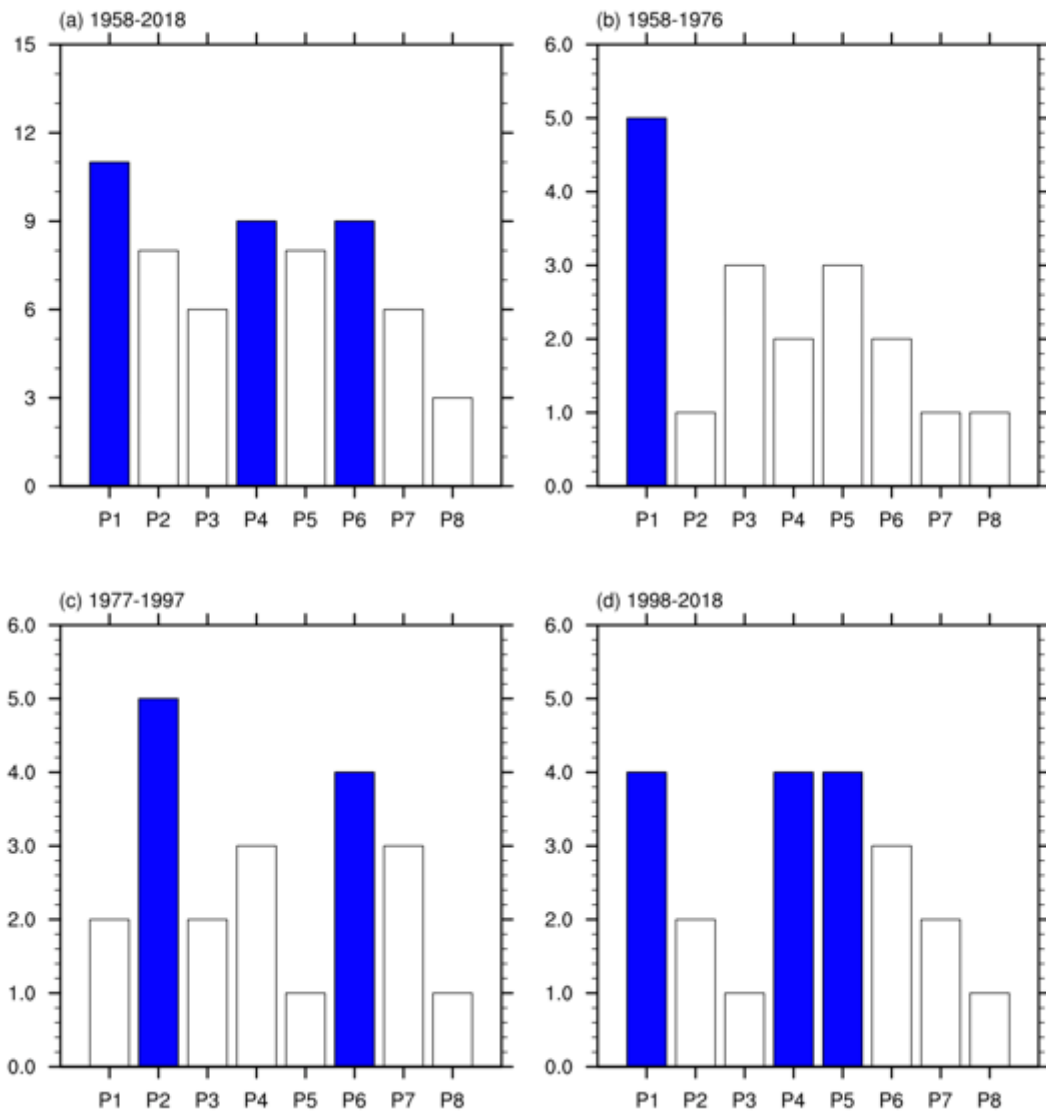


Figure 8

Same as Fig. 7 but for late winter (February–March) averages.